

CHAPTER

8

FLOW IN PIPES

Fluid flow in circular and noncircular pipes is commonly encountered in practice. The hot and cold water that we use in our homes is pumped through pipes. Water in a city is distributed by extensive piping networks. Oil and natural gas are transported hundreds of miles by large pipelines. Blood is carried throughout our bodies by arteries and veins. The cooling water in an engine is transported by hoses to the pipes in the radiator where it is cooled as it flows. Thermal energy in a hydronic space heating system is transferred to the circulating water in the boiler, and then it is transported to the desired locations through pipes.

Fluid flow is classified as *external* and *internal*, depending on whether the fluid is forced to flow over a surface or in a conduit. Internal and external flows exhibit very different characteristics. In this chapter we consider *internal flow* where the conduit is completely filled with the fluid, and flow is driven primarily by a pressure difference. This should not be confused with *open-channel flow* where the conduit is partially filled by the fluid and thus the flow is partially bounded by solid surfaces, as in an irrigation ditch, and flow is driven by gravity alone.

We start this chapter with a general physical description of internal flow and the *velocity boundary layer*. We continue with a discussion of the dimensionless *Reynolds number* and its physical significance. We then discuss the characteristics of flow inside pipes and introduce the *pressure drop* correlations associated with it for both laminar and turbulent flows. Then we present the minor losses and determine the pressure drop and pumping power requirements for real-world piping systems. Finally, we present an overview of flow measurement devices.

■■■■■■■■
OBJECTIVES

When you finish reading this chapter, you should be able to

- Have a deeper understanding of laminar and turbulent flow in pipes and the analysis of fully developed flow
- Calculate the major and minor losses associated with pipe flow in piping networks and determine the pumping power requirements
- Understand the different velocity and flow rate measurement techniques and learn their advantages and disadvantages

8-1 ■ INTRODUCTION

Liquid or gas flow through *pipes* or *ducts* is commonly used in heating and cooling applications and fluid distribution networks. The fluid in such applications is usually forced to flow by a fan or pump through a flow section. We pay particular attention to *friction*, which is directly related to the *pressure drop* and *head loss* during flow through pipes and ducts. The pressure drop is then used to determine the pumping power requirement. A typical piping system involves pipes of different diameters connected to each other by various fittings or elbows to route the fluid, valves to control the flow rate, and pumps to pressurize the fluid.

The terms *pipe*, *duct*, and *conduit* are usually used interchangeably for flow sections. In general, flow sections of circular cross section are referred to as *pipes* (especially when the fluid is a liquid), and flow sections of non-circular cross section as *ducts* (especially when the fluid is a gas). Small-diameter pipes are usually referred to as *tubes*. Given this uncertainty, we will use more descriptive phrases (such as *a circular pipe* or *a rectangular duct*) whenever necessary to avoid any misunderstandings.

You have probably noticed that most fluids, especially liquids, are transported in *circular pipes*. This is because pipes with a circular cross section can withstand large pressure differences between the inside and the outside without undergoing significant distortion. *Noncircular pipes* are usually used in applications such as the heating and cooling systems of buildings where the pressure difference is relatively small, the manufacturing and installation costs are lower, and the available space is limited for ductwork (Fig. 8-1).

Although the theory of fluid flow is reasonably well understood, theoretical solutions are obtained only for a few simple cases such as fully developed laminar flow in a circular pipe. Therefore, we must rely on experimental results and empirical relations for most fluid flow problems rather than closed-form analytical solutions. Noting that the experimental results are obtained under carefully controlled laboratory conditions and that no two systems are exactly alike, we must not be so naive as to view the results obtained as “exact.” An error of 10 percent (or more) in friction factors calculated using the relations in this chapter is the “norm” rather than the “exception.”

The fluid velocity in a pipe changes from *zero* at the surface because of the no-slip condition to a maximum at the pipe center. In fluid flow, it is convenient to work with an *average velocity* V_{avg} , which remains constant in incompressible flow when the cross-sectional area of the pipe is constant (Fig. 8-2). The average velocity in heating and cooling applications may change somewhat because of changes in density with temperature. But, in practice, we evaluate the fluid properties at some average temperature and treat them as constants. The convenience of working with constant properties usually more than justifies the slight loss in accuracy.

Also, the friction between the fluid particles in a pipe does cause a slight rise in fluid temperature as a result of the mechanical energy being converted to sensible thermal energy. But this temperature rise due to *frictional heating* is usually too small to warrant any consideration in calculations and thus is disregarded. For example, in the absence of any heat transfer, no

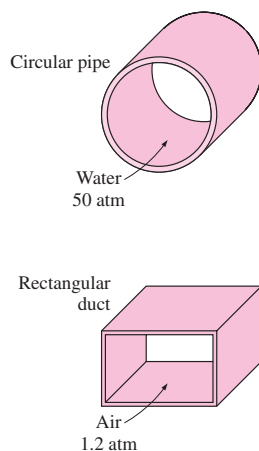


FIGURE 8-1

Circular pipes can withstand large pressure differences between the inside and the outside without undergoing any significant distortion, but noncircular pipes cannot.

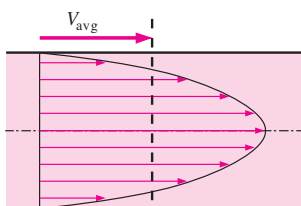


FIGURE 8-2

Average velocity V_{avg} is defined as the average speed through a cross section. For fully developed laminar pipe flow, V_{avg} is half of maximum velocity.

noticeable difference can be detected between the inlet and outlet temperatures of water flowing in a pipe. The primary consequence of friction in fluid flow is pressure drop, and thus any significant temperature change in the fluid is due to heat transfer.

The value of the average velocity V_{avg} at some streamwise cross-section is determined from the requirement that the *conservation of mass* principle be satisfied (Fig. 8–2). That is,

$$\dot{m} = \rho V_{\text{avg}} A_c = \int_{A_c} \rho u(r) dA_c \quad (8-1)$$

where \dot{m} is the mass flow rate, ρ is the density, A_c is the cross-sectional area, and $u(r)$ is the velocity profile. Then the average velocity for incompressible flow in a circular pipe of radius R can be expressed as

$$V_{\text{avg}} = \frac{\int_{A_c} \rho u(r) dA_c}{\rho A_c} = \frac{\int_0^R \rho u(r) 2\pi r dr}{\rho \pi R^2} = \frac{2}{R^2} \int_0^R u(r) r dr \quad (8-2)$$

Therefore, when we know the flow rate or the velocity profile, the average velocity can be determined easily.

8–2 ■ LAMINAR AND TURBULENT FLOWS

If you have been around smokers, you probably noticed that the cigarette smoke rises in a smooth plume for the first few centimeters and then starts fluctuating randomly in all directions as it continues its rise. Other plumes behave similarly (Fig. 8–3). Likewise, a careful inspection of flow in a pipe reveals that the fluid flow is streamlined at low velocities but turns chaotic as the velocity is increased above a critical value, as shown in Fig. 8–4. The flow regime in the first case is said to be **laminar**, characterized by *smooth streamlines* and *highly ordered motion*, and **turbulent** in the second case, where it is characterized by *velocity fluctuations* and *highly disordered motion*. The **transition** from laminar to turbulent flow does not occur suddenly; rather, it occurs over some region in which the flow fluctuates between laminar and turbulent flows before it becomes fully turbulent. Most flows encountered in practice are turbulent. Laminar flow is encountered when highly viscous fluids such as oils flow in small pipes or narrow passages.

We can verify the existence of these laminar, transitional, and turbulent flow regimes by injecting some dye streaks into the flow in a glass pipe, as the British engineer Osborne Reynolds (1842–1912) did over a century ago. We observe that the dye streak forms a *straight and smooth line* at low velocities when the flow is laminar (we may see some blurring because of molecular diffusion), has *bursts of fluctuations* in the transitional regime, and *zigzags rapidly and randomly* when the flow becomes fully turbulent. These zigzags and the dispersion of the dye are indicative of the fluctuations in the main flow and the rapid mixing of fluid particles from adjacent layers.

The *intense mixing* of the fluid in turbulent flow as a result of rapid fluctuations enhances momentum transfer between fluid particles, which increases the friction force on the surface and thus the required pumping power. The friction factor reaches a maximum when the flow becomes fully turbulent.

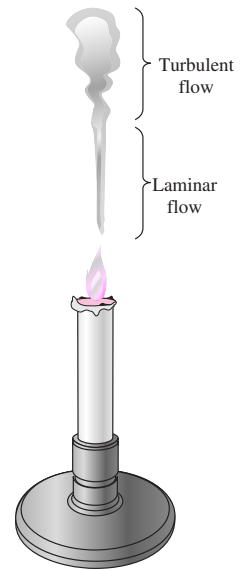


FIGURE 8–3
Laminar and turbulent flow regimes of candle smoke.

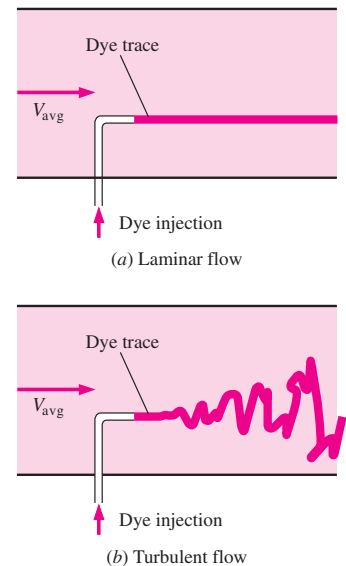


FIGURE 8–4
The behavior of colored fluid injected into the flow in laminar and turbulent flows in a pipe.

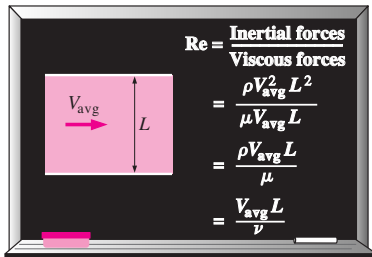


FIGURE 8-5
The Reynolds number can be viewed as the ratio of inertial forces to viscous forces acting on a fluid element.

Reynolds Number

The transition from laminar to turbulent flow depends on the *geometry*, *surface roughness*, *flow velocity*, *surface temperature*, and *type of fluid*, among other things. After exhaustive experiments in the 1880s, Osborne Reynolds discovered that the flow regime depends mainly on the ratio of *inertial forces* to *viscous forces* in the fluid. This ratio is called the **Reynolds number** and is expressed for internal flow in a circular pipe as (Fig. 8-5)

$$Re = \frac{\text{Inertial forces}}{\text{Viscous forces}} = \frac{V_{avg} D}{\nu} = \frac{\rho V_{avg} D}{\mu} \tag{8-3}$$

where V_{avg} = average flow velocity (m/s), D = characteristic length of the geometry (diameter in this case, in m), and $\nu = \mu/\rho$ = kinematic viscosity of the fluid (m²/s). Note that the Reynolds number is a *dimensionless* quantity (Chap. 7). Also, kinematic viscosity has the unit m²/s, and can be viewed as *viscous diffusivity* or *diffusivity for momentum*.

At large Reynolds numbers, the inertial forces, which are proportional to the fluid density and the square of the fluid velocity, are large relative to the viscous forces, and thus the viscous forces cannot prevent the random and rapid fluctuations of the fluid. At *small* or *moderate* Reynolds numbers, however, the viscous forces are large enough to suppress these fluctuations and to keep the fluid “in line.” Thus the flow is *turbulent* in the first case and *laminar* in the second.

The Reynolds number at which the flow becomes turbulent is called the **critical Reynolds number**, Re_{cr} . The value of the critical Reynolds number is different for different geometries and flow conditions. For internal flow in a circular pipe, the generally accepted value of the critical Reynolds number is $Re_{cr} = 2300$.

For flow through noncircular pipes, the Reynolds number is based on the **hydraulic diameter** D_h defined as (Fig. 8-6)

Hydraulic diameter:
$$D_h = \frac{4A_c}{p} \tag{8-4}$$

where A_c is the cross-sectional area of the pipe and p is its wetted perimeter. The hydraulic diameter is defined such that it reduces to ordinary diameter D for circular pipes,

Circular pipes:
$$D_h = \frac{4A_c}{p} = \frac{4(\pi D^2/4)}{\pi D} = D$$

It certainly is desirable to have precise values of Reynolds numbers for laminar, transitional, and turbulent flows, but this is not the case in practice. It turns out that the transition from laminar to turbulent flow also depends on the degree of disturbance of the flow by *surface roughness*, *pipe vibrations*, and *fluctuations in the flow*. Under most practical conditions, the flow in a circular pipe is laminar for $Re \lesssim 2300$, turbulent for $Re \gtrsim 4000$, and transitional in between. That is,

- $Re \lesssim 2300$ laminar flow
- $2300 \lesssim Re \lesssim 4000$ transitional flow
- $Re \gtrsim 4000$ turbulent flow

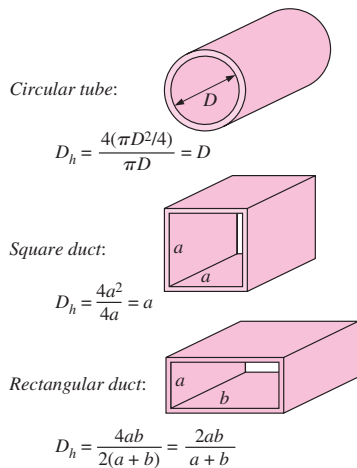


FIGURE 8-6
The hydraulic diameter $D_h = 4A_c/p$ is defined such that it reduces to ordinary diameter for circular tubes.

In transitional flow, the flow switches between laminar and turbulent randomly (Fig. 8–7). It should be kept in mind that laminar flow can be maintained at much higher Reynolds numbers in very smooth pipes by avoiding flow disturbances and pipe vibrations. In such carefully controlled experiments, laminar flow has been maintained at Reynolds numbers of up to 100,000.

8–3 ■ THE ENTRANCE REGION

Consider a fluid entering a circular pipe at a uniform velocity. Because of the no-slip condition, the fluid particles in the layer in contact with the surface of the pipe come to a complete stop. This layer also causes the fluid particles in the adjacent layers to slow down gradually as a result of friction. To make up for this velocity reduction, the velocity of the fluid at the mid-section of the pipe has to increase to keep the mass flow rate through the pipe constant. As a result, a velocity gradient develops along the pipe.

The region of the flow in which the effects of the viscous shearing forces caused by fluid viscosity are felt is called the **velocity boundary layer** or just the **boundary layer**. The hypothetical boundary surface divides the flow in a pipe into two regions: the **boundary layer region**, in which the viscous effects and the velocity changes are significant, and the **irrotational (core) flow region**, in which the frictional effects are negligible and the velocity remains essentially constant in the radial direction.

The thickness of this boundary layer increases in the flow direction until the boundary layer reaches the pipe center and thus fills the entire pipe, as shown in Fig. 8–8. The region from the pipe inlet to the point at which the boundary layer merges at the centerline is called the **hydrodynamic entrance region**, and the length of this region is called the **hydrodynamic entry length** L_h . Flow in the entrance region is called *hydrodynamically developing flow* since this is the region where the velocity profile develops. The region beyond the entrance region in which the velocity profile is fully developed and remains unchanged is called the **hydrodynamically fully developed region**. The flow is said to be **fully developed** when the normalized temperature profile remains unchanged as well. Hydrodynamically developed flow is equivalent to fully developed flow when the fluid in the pipe is not heated or cooled since the fluid temperature in this case remains

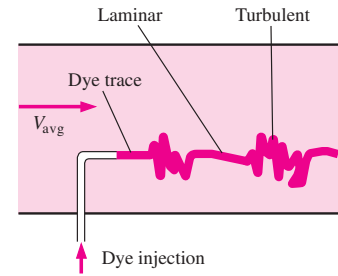


FIGURE 8–7
In the transitional flow region of $2300 \leq Re \leq 4000$, the flow switches between laminar and turbulent randomly.

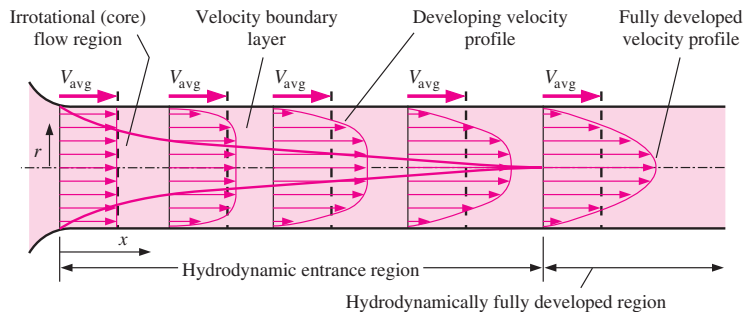


FIGURE 8–8
The development of the velocity boundary layer in a pipe. (The developed average velocity profile is parabolic in laminar flow, as shown, but somewhat flatter or fuller in turbulent flow.)

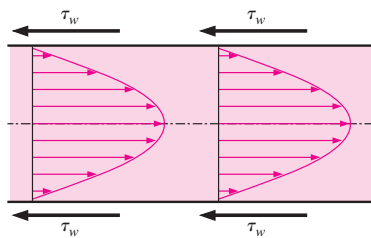


FIGURE 8-9
In the fully developed flow region of a pipe, the velocity profile does not change downstream, and thus the wall shear stress remains constant as well.

essentially constant throughout. The velocity profile in the fully developed region is *parabolic* in laminar flow and somewhat *flatter* (or *fuller*) in turbulent flow due to eddy motion and more vigorous mixing in the radial direction. The time-averaged velocity profile remains unchanged when the flow is fully developed, and thus

$$\text{Hydrodynamically fully developed: } \frac{\partial u(r, x)}{\partial x} = 0 \rightarrow u = u(r) \quad (8-5)$$

The shear stress at the pipe wall τ_w is related to the slope of the velocity profile at the surface. Noting that the velocity profile remains unchanged in the hydrodynamically fully developed region, the wall shear stress also remains constant in that region (Fig. 8-9).

Consider fluid flow in the hydrodynamic entrance region of a pipe. The wall shear stress is the *highest* at the pipe inlet where the thickness of the boundary layer is smallest, and decreases gradually to the fully developed value, as shown in Fig. 8-10. Therefore, the pressure drop is *higher* in the entrance regions of a pipe, and the effect of the entrance region is always to *increase* the average friction factor for the entire pipe. This increase may be significant for short pipes but is negligible for long ones.

Entry Lengths

The hydrodynamic entry length is usually taken to be the distance from the pipe entrance to where the wall shear stress (and thus the friction factor) reaches within about 2 percent of the fully developed value. In *laminar flow*, the hydrodynamic entry length is given approximately as [see Kays and Crawford (1993) and Shah and Bhatti (1987)]

$$L_{h, \text{laminar}} \cong 0.05\text{Re}D \quad (8-6)$$

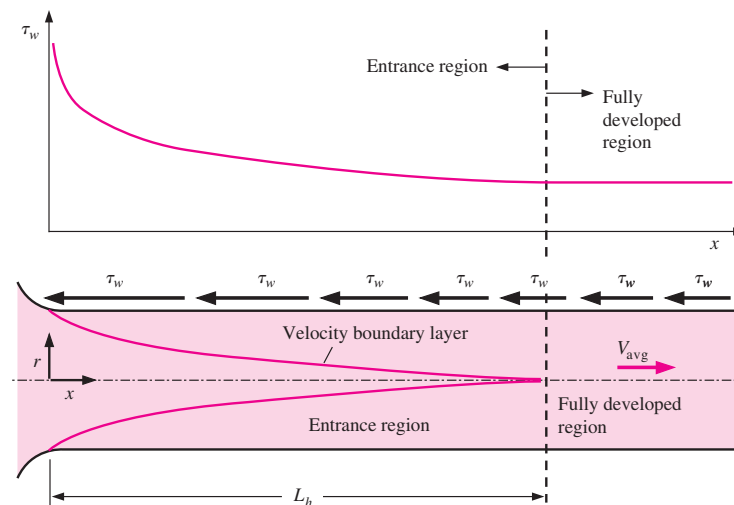


FIGURE 8-10
The variation of wall shear stress in the flow direction for flow in a pipe from the entrance region into the fully developed region.

For $Re = 20$, the hydrodynamic entry length is about the size of the diameter, but increases linearly with velocity. In the limiting laminar case of $Re = 2300$, the hydrodynamic entry length is $115D$.

In *turbulent flow*, the intense mixing during random fluctuations usually overshadows the effects of molecular diffusion. The hydrodynamic entry length for turbulent flow can be approximated as [see Bhatti and Shah (1987) and Zhi-qing (1982)]

$$L_{h, \text{turbulent}} = 1.359DRe_D^{1/4} \quad (8-7)$$

The entry length is much shorter in turbulent flow, as expected, and its dependence on the Reynolds number is weaker. In many pipe flows of practical engineering interest, the entrance effects become insignificant beyond a pipe length of 10 diameters, and the hydrodynamic entry length is approximated as

$$L_{h, \text{turbulent}} \approx 10D \quad (8-8)$$

Precise correlations for calculating the frictional head losses in entrance regions are available in the literature. However, the pipes used in practice are usually several times the length of the entrance region, and thus the flow through the pipes is often assumed to be fully developed for the entire length of the pipe. This simplistic approach gives *reasonable* results for long pipes but sometimes poor results for short ones since it underpredicts the wall shear stress and thus the friction factor.

8-4 ■ LAMINAR FLOW IN PIPES

We mentioned in Section 8-2 that flow in pipes is laminar for $Re \leq 2300$, and that the flow is fully developed if the pipe is sufficiently long (relative to the entry length) so that the entrance effects are negligible. In this section we consider the steady laminar flow of an incompressible fluid with constant properties in the fully developed region of a straight circular pipe. We obtain the momentum equation by applying a momentum balance to a differential volume element, and obtain the velocity profile by solving it. Then we use it to obtain a relation for the friction factor. An important aspect of the analysis here is that it is one of the few available for viscous flow.

In fully developed laminar flow, each fluid particle moves at a constant axial velocity along a streamline and the velocity profile $u(r)$ remains unchanged in the flow direction. There is no motion in the radial direction, and thus the velocity component in the direction normal to flow is everywhere zero. There is no acceleration since the flow is steady and fully developed.

Now consider a ring-shaped differential volume element of radius r ; thickness dr ; and length dx oriented coaxially with the pipe, as shown in Fig. 8-11. The volume element involves only pressure and viscous effects and thus the pressure and shear forces must balance each other. The pressure force acting on a submerged plane surface is the product of the pressure at the centroid of the surface and the surface area. A force balance on the volume element in the flow direction gives

$$(2\pi r dr P)_x - (2\pi r dr P)_{x+dx} + (2\pi r dx \tau)_r - (2\pi r dx \tau)_{r+dr} = 0 \quad (8-9)$$

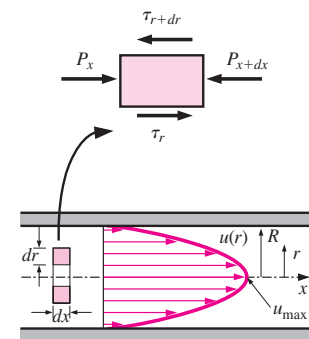
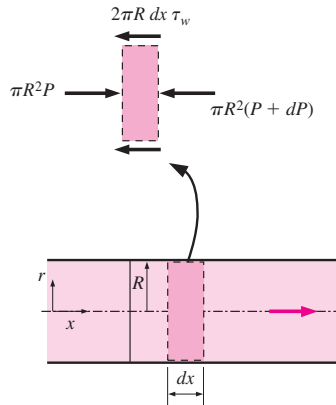


FIGURE 8-11

Free-body diagram of a ring-shaped differential fluid element of radius r , thickness dr , and length dx oriented coaxially with a horizontal pipe in fully developed laminar flow.



Force balance:

$$\pi R^2 P - \pi R^2 (P + dP) - 2\pi R dx \tau_w = 0$$

Simplifying:

$$\frac{dP}{dx} = -\frac{2\tau_w}{R}$$

FIGURE 8-12

Free-body diagram of a fluid disk element of radius R and length dx in fully developed laminar flow in a horizontal pipe.

which indicates that in fully developed flow in a horizontal pipe, the viscous and pressure forces balance each other. Dividing by $2\pi r dx$ and rearranging,

$$r \frac{P_{x+dx} - P_x}{dx} + \frac{(r\tau)_{r+dr} - (r\tau)_r}{dr} = 0 \quad (8-10)$$

Taking the limit as $dr, dx \rightarrow 0$ gives

$$r \frac{dP}{dx} + \frac{d(r\tau)}{dr} = 0 \quad (8-11)$$

Substituting $\tau = -\mu(du/dr)$ and taking $\mu = \text{constant}$ gives the desired equation,

$$\frac{\mu}{r} \frac{d}{dr} \left(r \frac{du}{dr} \right) = \frac{dP}{dx} \quad (8-12)$$

The quantity du/dr is negative in pipe flow, and the negative sign is included to obtain positive values for τ . (Or, $du/dr = -du/dy$ since $y = R - r$.) The left side of Eq. 8-12 is a function of r , and the right side is a function of x . The equality must hold for any value of r and x , and an equality of the form $f(r) = g(x)$ can be satisfied only if both $f(r)$ and $g(x)$ are equal to the same constant. Thus we conclude that $dP/dx = \text{constant}$. This can be verified by writing a force balance on a volume element of radius R and thickness dx (a slice of the pipe), which gives (Fig. 8-12)

$$\frac{dP}{dx} = -\frac{2\tau_w}{R} \quad (8-13)$$

Here τ_w is constant since the viscosity and the velocity profile are constants in the fully developed region. Therefore, $dP/dx = \text{constant}$.

Equation 8-12 can be solved by rearranging and integrating it twice to give

$$u(r) = \frac{1}{4\mu} \left(\frac{dP}{dx} \right) r^2 + C_1 \ln r + C_2 \quad (8-14)$$

The velocity profile $u(r)$ is obtained by applying the boundary conditions $\partial u/\partial r = 0$ at $r = 0$ (because of symmetry about the centerline) and $u = 0$ at $r = R$ (the no-slip condition at the pipe surface). We get

$$u(r) = -\frac{R^2}{4\mu} \left(\frac{dP}{dx} \right) \left(1 - \frac{r^2}{R^2} \right) \quad (8-15)$$

Therefore, the velocity profile in fully developed laminar flow in a pipe is *parabolic* with a maximum at the centerline and minimum (zero) at the pipe wall. Also, the axial velocity u is positive for any r , and thus the axial pressure gradient dP/dx must be negative (i.e., pressure must decrease in the flow direction because of viscous effects).

The average velocity is determined from its definition by substituting Eq. 8-15 into Eq. 8-2, and performing the integration. It gives

$$V_{\text{avg}} = \frac{2}{R^2} \int_0^R u(r)r dr = \frac{-2}{R^2} \int_0^R \frac{R^2}{4\mu} \left(\frac{dP}{dx} \right) \left(1 - \frac{r^2}{R^2} \right) r dr = -\frac{R^2}{8\mu} \left(\frac{dP}{dx} \right) \quad (8-16)$$

Combining the last two equations, the velocity profile is rewritten as

$$u(r) = 2V_{\text{avg}} \left(1 - \frac{r^2}{R^2} \right) \quad (8-17)$$

This is a convenient form for the velocity profile since V_{avg} can be determined easily from the flow rate information.

The maximum velocity occurs at the centerline and is determined from Eq. 8-17 by substituting $r = 0$,

$$u_{\text{max}} = 2V_{\text{avg}} \quad (8-18)$$

Therefore, *the average velocity in fully developed laminar pipe flow is one-half of the maximum velocity.*

Pressure Drop and Head Loss

A quantity of interest in the analysis of pipe flow is the *pressure drop* ΔP since it is directly related to the power requirements of the fan or pump to maintain flow. We note that $dP/dx = \text{constant}$, and integrating from $x = x_1$ where the pressure is P_1 to $x = x_1 + L$ where the pressure is P_2 gives

$$\frac{dP}{dx} = \frac{P_2 - P_1}{L} \quad (8-19)$$

Substituting Eq. 8-19 into the V_{avg} expression in Eq. 8-16, the pressure drop can be expressed as

$$\text{Laminar flow:} \quad \Delta P = P_1 - P_2 = \frac{8\mu LV_{\text{avg}}}{R^2} = \frac{32\mu LV_{\text{avg}}}{D^2} \quad (8-20)$$

The symbol Δ is typically used to indicate the difference between the final and initial values, like $\Delta y = y_2 - y_1$. But in fluid flow, ΔP is used to designate pressure drop, and thus it is $P_1 - P_2$. A pressure drop due to viscous effects represents an irreversible pressure loss, and it is called **pressure loss** ΔP_L to emphasize that it is a *loss* (just like the head loss h_L , which is proportional to it).

Note from Eq. 8-20 that the pressure drop is proportional to the viscosity μ of the fluid, and ΔP would be zero if there were no friction. Therefore, the drop of pressure from P_1 to P_2 in this case is due entirely to viscous effects, and Eq. 8-20 represents the pressure loss ΔP_L when a fluid of viscosity μ flows through a pipe of constant diameter D and length L at average velocity V_{avg} .

In practice, it is found convenient to express the pressure loss for all types of fully developed internal flows (laminar or turbulent flows, circular or noncircular pipes, smooth or rough surfaces, horizontal or inclined pipes) as (Fig. 8-13)

$$\text{Pressure loss:} \quad \Delta P_L = f \frac{L}{D} \frac{\rho V_{\text{avg}}^2}{2} \quad (8-21)$$

where $\rho V_{\text{avg}}^2/2$ is the *dynamic pressure* and f is the **Darcy friction factor**,

$$f = \frac{8\tau_w}{\rho V_{\text{avg}}^2} \quad (8-22)$$

It is also called the **Darcy–Weisbach friction factor**, named after the Frenchman Henry Darcy (1803–1858) and the German Julius Weisbach (1806–1871), the two engineers who provided the greatest contribution in its development. It should not be confused with the *friction coefficient* C_f

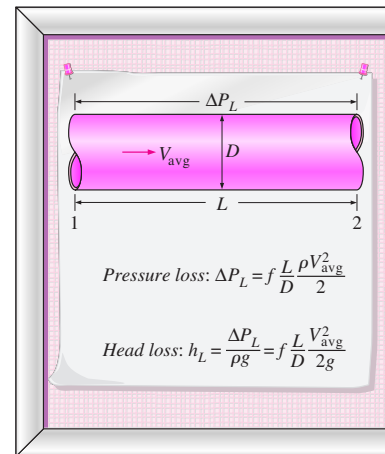


FIGURE 8-13

The relation for pressure loss (and head loss) is one of the most general relations in fluid mechanics, and it is valid for laminar or turbulent flows, circular or noncircular pipes, and pipes with smooth or rough surfaces.

[also called the *Fanning friction factor*, named after the American engineer John Fanning (1837–1911)], which is defined as $C_f = 2\tau_w/(\rho V_{avg}^2) = f/4$.

Setting Eqs. 8–20 and 8–21 equal to each other and solving for f gives the friction factor for fully developed laminar flow in a circular pipe,

$$\text{Circular pipe, laminar: } f = \frac{64\mu}{\rho D V_{avg}} = \frac{64}{Re} \tag{8-23}$$

This equation shows that *in laminar flow, the friction factor is a function of the Reynolds number only and is independent of the roughness of the pipe surface.*

In the analysis of piping systems, pressure losses are commonly expressed in terms of the *equivalent fluid column height*, called the **head loss** h_L . Noting from fluid statics that $\Delta P = \rho gh$ and thus a pressure difference of ΔP corresponds to a fluid height of $h = \Delta P/\rho g$, the *pipe head loss* is obtained by dividing ΔP_L by ρg to give

$$\text{Head loss: } h_L = \frac{\Delta P_L}{\rho g} = f \frac{L}{D} \frac{V_{avg}^2}{2g} \tag{8-24}$$

The head loss h_L represents *the additional height that the fluid needs to be raised by a pump in order to overcome the frictional losses in the pipe.* The head loss is caused by viscosity, and it is directly related to the wall shear stress. Equations 8–21 and 8–24 are valid for both laminar and turbulent flows in both circular and noncircular pipes, but Eq. 8–23 is valid only for fully developed laminar flow in circular pipes.

Once the pressure loss (or head loss) is known, the required pumping power to overcome the pressure loss is determined from

$$\dot{W}_{pump,L} = \dot{V} \Delta P_L = \dot{V} \rho g h_L = \dot{m} g h_L \tag{8-25}$$

where \dot{V} is the volume flow rate and \dot{m} is the mass flow rate.

The average velocity for laminar flow in a horizontal pipe is, from Eq. 8–20,

$$\text{Horizontal pipe: } V_{avg} = \frac{(P_1 - P_2)R^2}{8\mu L} = \frac{(P_1 - P_2)D^2}{32\mu L} = \frac{\Delta P D^2}{32\mu L} \tag{8-26}$$

Then the volume flow rate for laminar flow through a horizontal pipe of diameter D and length L becomes

$$\dot{V} = V_{avg} A_c = \frac{(P_1 - P_2)R^2}{8\mu L} \pi R^2 = \frac{(P_1 - P_2)\pi D^4}{128\mu L} = \frac{\Delta P \pi D^4}{128\mu L} \tag{8-27}$$

This equation is known as **Poiseuille’s law**, and this flow is called *Hagen–Poiseuille flow* in honor of the works of G. Hagen (1797–1884) and J. Poiseuille (1799–1869) on the subject. Note from Eq. 8–27 that *for a specified flow rate, the pressure drop and thus the required pumping power is proportional to the length of the pipe and the viscosity of the fluid, but it is inversely proportional to the fourth power of the radius (or diameter) of the pipe.* Therefore, the pumping power requirement for a piping system can be reduced by a factor of 16 by doubling the pipe diameter (Fig. 8–14). Of course the benefits of the reduction in the energy costs must be weighed against the increased cost of construction due to using a larger-diameter pipe.

The pressure drop ΔP equals the pressure loss ΔP_L in the case of a horizontal pipe, but this is not the case for inclined pipes or pipes with variable cross-sectional area. This can be demonstrated by writing the energy

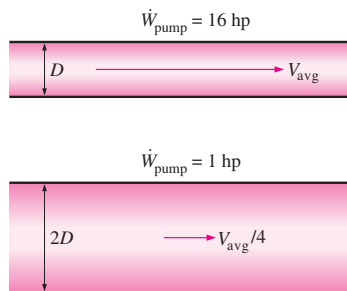


FIGURE 8–14 The pumping power requirement for a laminar flow piping system can be reduced by a factor of 16 by doubling the pipe diameter.

equation for steady, incompressible one-dimensional flow in terms of heads as (see Chap. 5)

$$\frac{P_1}{\rho g} + \alpha_1 \frac{V_1^2}{2g} + z_1 + h_{\text{pump},u} = \frac{P_2}{\rho g} + \alpha_2 \frac{V_2^2}{2g} + z_2 + h_{\text{turbine},e} + h_L \quad (8-28)$$

where $h_{\text{pump},u}$ is the useful pump head delivered to the fluid, $h_{\text{turbine},e}$ is the turbine head extracted from the fluid, h_L is the irreversible head loss between sections 1 and 2, V_1 and V_2 are the average velocities at sections 1 and 2, respectively, and α_1 and α_2 are the *kinetic energy correction factors* at sections 1 and 2 (it can be shown that $\alpha = 2$ for fully developed laminar flow and about 1.05 for fully developed turbulent flow). Equation 8-28 can be rearranged as

$$P_1 - P_2 = \rho(\alpha_2 V_2^2 - \alpha_1 V_1^2)/2 + \rho g[(z_2 - z_1) + h_{\text{turbine},e} - h_{\text{pump},u} + h_L] \quad (8-29)$$

Therefore, the pressure drop $\Delta P = P_1 - P_2$ and pressure loss $\Delta P_L = \rho g h_L$ for a given flow section are equivalent if (1) the flow section is horizontal so that there are no hydrostatic or gravity effects ($z_1 = z_2$), (2) the flow section does not involve any work devices such as a pump or a turbine since they change the fluid pressure ($h_{\text{pump},u} = h_{\text{turbine},e} = 0$), (3) the cross-sectional area of the flow section is constant and thus the average flow velocity is constant ($V_1 = V_2$), and (4) the velocity profiles at sections 1 and 2 are the same shape ($\alpha_1 = \alpha_2$).

Inclined Pipes

Relations for inclined pipes can be obtained in a similar manner from a force balance in the direction of flow. The only additional force in this case is the component of the fluid weight in the flow direction, whose magnitude is

$$W_x = W \sin \theta = \rho g V_{\text{element}} \sin \theta = \rho g (2\pi r dr dx) \sin \theta \quad (8-30)$$

where θ is the angle between the horizontal and the flow direction (Fig. 8-15). The force balance in Eq. 8-9 now becomes

$$(2\pi r dr P)_x - (2\pi r dr P)_{x+dx} + (2\pi r dx \tau)_r - (2\pi r dx \tau)_{r+dr} - \rho g (2\pi r dr dx) \sin \theta = 0 \quad (8-31)$$

which results in the differential equation

$$\frac{\mu}{r} \frac{d}{dr} \left(r \frac{du}{dr} \right) = \frac{dP}{dx} + \rho g \sin \theta \quad (8-32)$$

Following the same solution procedure, the velocity profile can be shown to be

$$u(r) = -\frac{R^2}{4\mu} \left(\frac{dP}{dx} + \rho g \sin \theta \right) \left(1 - \frac{r^2}{R^2} \right) \quad (8-33)$$

It can also be shown that the *average velocity* and the *volume flow rate* relations for laminar flow through inclined pipes are, respectively,

$$V_{\text{avg}} = \frac{(\Delta P - \rho g L \sin \theta) D^2}{32\mu L} \quad \text{and} \quad \dot{V} = \frac{(\Delta P - \rho g L \sin \theta) \pi D^4}{128\mu L} \quad (8-34)$$

which are identical to the corresponding relations for horizontal pipes, except that ΔP is replaced by $\Delta P - \rho g L \sin \theta$. Therefore, the results already obtained for horizontal pipes can also be used for inclined pipes provided that ΔP is replaced by $\Delta P - \rho g L \sin \theta$ (Fig. 8-16). Note that $\theta > 0$ and thus $\sin \theta > 0$ for uphill flow, and $\theta < 0$ and thus $\sin \theta < 0$ for downhill flow.

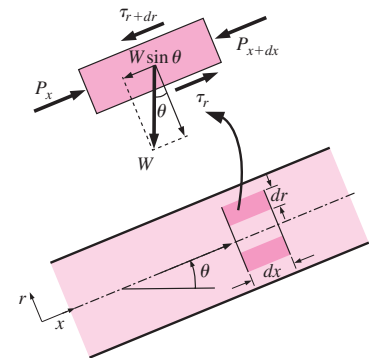


FIGURE 8-15 Free-body diagram of a ring-shaped differential fluid element of radius r , thickness dr , and length dx oriented coaxially with an inclined pipe in fully developed laminar flow.

<input type="radio"/>	
<input type="radio"/>	Horizontal pipe: $\dot{V} = \frac{\Delta P \pi D^4}{128\mu L}$
	Inclined pipe: $\dot{V} = \frac{(\Delta P - \rho g L \sin \theta) \pi D^4}{128\mu L}$
	Uphill flow: $\theta > 0$ and $\sin \theta > 0$
<input type="radio"/>	Downhill flow: $\theta < 0$ and $\sin \theta < 0$
<input type="radio"/>	
<input type="radio"/>	

FIGURE 8-16 The relations developed for fully developed laminar flow through horizontal pipes can also be used for inclined pipes by replacing ΔP with $\Delta P - \rho g L \sin \theta$.

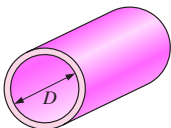
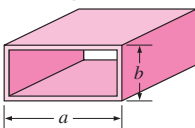
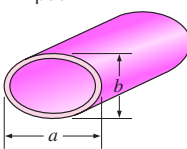
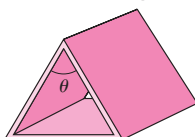
In inclined pipes, the combined effect of pressure difference and gravity drives the flow. Gravity helps downhill flow but opposes uphill flow. Therefore, much greater pressure differences need to be applied to maintain a specified flow rate in uphill flow although this becomes important only for liquids, because the density of gases is generally low. In the special case of *no flow* ($\dot{V} = 0$), we have $\Delta P = \rho g L \sin \theta$, which is what we would obtain from fluid statics (Chap. 3).

Laminar Flow in Noncircular Pipes

The friction factor f relations are given in Table 8–1 for *fully developed laminar flow* in pipes of various cross sections. The Reynolds number for flow in these pipes is based on the hydraulic diameter $D_h = 4A_c/p$, where A_c is the cross-sectional area of the pipe and p is its wetted perimeter.

TABLE 8–1

Friction factor for fully developed *laminar flow* in pipes of various cross sections ($D_h = 4A_c/p$ and $Re = V_{avg} D_h/\nu$)

Tube Geometry	a/b or θ°	Friction Factor f
Circle	—	64.00/Re
		
Rectangle	a/b	
	1	56.92/Re
	2	62.20/Re
	3	68.36/Re
	4	72.92/Re
	6	78.80/Re
	8	82.32/Re
	∞	96.00/Re
Ellipse	a/b	
	1	64.00/Re
	2	67.28/Re
	4	72.96/Re
	8	76.60/Re
	16	78.16/Re
Isosceles triangle	θ	
	10°	50.80/Re
	30°	52.28/Re
	60°	53.32/Re
	90°	52.60/Re
	120°	50.96/Re

EXAMPLE 8-1 Flow Rates in Horizontal and Inclined Pipes

Oil at 20°C ($\rho = 888 \text{ kg/m}^3$ and $\mu = 0.800 \text{ kg/m} \cdot \text{s}$) is flowing steadily through a 5-cm-diameter 40-m-long pipe (Fig. 8-17). The pressure at the pipe inlet and outlet are measured to be 745 and 97 kPa, respectively. Determine the flow rate of oil through the pipe assuming the pipe is (a) horizontal, (b) inclined 15° upward, (c) inclined 15° downward. Also verify that the flow through the pipe is laminar.

SOLUTION The pressure readings at the inlet and outlet of a pipe are given. The flow rates are to be determined for three different orientations, and the flow is to be shown to be laminar.

Assumptions 1 The flow is steady and incompressible. 2 The entrance effects are negligible, and thus the flow is fully developed. 3 The pipe involves no components such as bends, valves, and connectors. 4 The piping section involves no work devices such as a pump or a turbine.

Properties The density and dynamic viscosity of oil are given to be $\rho = 888 \text{ kg/m}^3$ and $\mu = 0.800 \text{ kg/m} \cdot \text{s}$, respectively.

Analysis The pressure drop across the pipe and the pipe cross-sectional area are

$$\Delta P = P_1 - P_2 = 745 - 97 = 648 \text{ kPa}$$

$$A_c = \pi D^2/4 = \pi(0.05 \text{ m})^2/4 = 0.001963 \text{ m}^2$$

(a) The flow rate for all three cases can be determined from Eq. 8-34,

$$\dot{V} = \frac{(\Delta P - \rho g L \sin \theta) \pi D^4}{128 \mu L}$$

where θ is the angle the pipe makes with the horizontal. For the horizontal case, $\theta = 0$ and thus $\sin \theta = 0$. Therefore,

$$\begin{aligned} \dot{V}_{\text{horiz}} &= \frac{\Delta P \pi D^4}{128 \mu L} = \frac{(648 \text{ kPa}) \pi (0.05 \text{ m})^4}{128(0.800 \text{ kg/m} \cdot \text{s})(40 \text{ m})} \left(\frac{1000 \text{ N/m}^2}{1 \text{ kPa}} \right) \left(\frac{1 \text{ kg} \cdot \text{m/s}^2}{1 \text{ N}} \right) \\ &= \mathbf{0.00311 \text{ m}^3/\text{s}} \end{aligned}$$

(b) For uphill flow with an inclination of 15°, we have $\theta = +15^\circ$, and

$$\begin{aligned} \dot{V}_{\text{uphill}} &= \frac{(\Delta P - \rho g L \sin \theta) \pi D^4}{128 \mu L} \\ &= \frac{[648,000 \text{ Pa} - (888 \text{ kg/m}^3)(9.81 \text{ m/s}^2)(40 \text{ m}) \sin 15^\circ] \pi (0.05 \text{ m})^4}{128(0.800 \text{ kg/m} \cdot \text{s})(40 \text{ m})} \left(\frac{1 \text{ kg} \cdot \text{m/s}^2}{1 \text{ Pa} \cdot \text{m}^2} \right) \\ &= \mathbf{0.00267 \text{ m}^3/\text{s}} \end{aligned}$$

(c) For downhill flow with an inclination of 15°, we have $\theta = -15^\circ$, and

$$\begin{aligned} \dot{V}_{\text{downhill}} &= \frac{(\Delta P - \rho g L \sin \theta) \pi D^4}{128 \mu L} \\ &= \frac{[648,000 \text{ Pa} - (888 \text{ kg/m}^3)(9.81 \text{ m/s}^2)(40 \text{ m}) \sin(-15^\circ)] \pi (0.05 \text{ m})^4}{128(0.800 \text{ kg/m} \cdot \text{s})(40 \text{ m})} \left(\frac{1 \text{ kg} \cdot \text{m/s}^2}{1 \text{ Pa} \cdot \text{m}^2} \right) \\ &= \mathbf{0.00354 \text{ m}^3/\text{s}} \end{aligned}$$

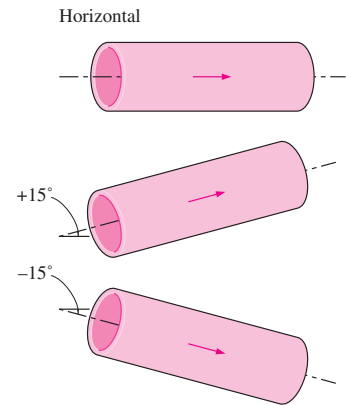


FIGURE 8-17
Schematic for Example 8-1.

The flow rate is the highest for the downhill flow case, as expected. The average fluid velocity and the Reynolds number in this case are

$$V_{\text{avg}} = \frac{\dot{V}}{A_c} = \frac{0.00354 \text{ m}^3/\text{s}}{0.001963 \text{ m}^2} = 1.80 \text{ m/s}$$

$$\text{Re} = \frac{\rho V_{\text{avg}} D}{\mu} = \frac{(888 \text{ kg/m}^3)(1.80 \text{ m/s})(0.05 \text{ m})}{0.800 \text{ kg/m} \cdot \text{s}} = 100$$

which is much less than 2300. Therefore, the flow is *laminar* for all three cases and the analysis is valid.

Discussion Note that the flow is driven by the combined effect of pressure difference and gravity. As can be seen from the flow rates we calculated, gravity opposes uphill flow, but enhances downhill flow. Gravity has no effect on the flow rate in the horizontal case. Downhill flow can occur even in the absence of an applied pressure difference. For the case of $P_1 = P_2 = 97 \text{ kPa}$ (i.e., no applied pressure difference), the pressure throughout the entire pipe would remain constant at 97 Pa, and the fluid would flow through the pipe at a rate of $0.00043 \text{ m}^3/\text{s}$ under the influence of gravity. The flow rate increases as the tilt angle of the pipe from the horizontal is increased in the negative direction and would reach its maximum value when the pipe is vertical.

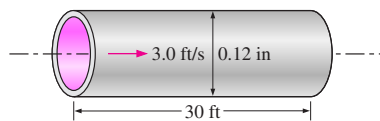


FIGURE 8–18
Schematic for Example 8–2.

EXAMPLE 8–2 Pressure Drop and Head Loss in a Pipe

Water at 40°F ($\rho = 62.42 \text{ lbm/ft}^3$ and $\mu = 1.038 \times 10^{-3} \text{ lbm/ft} \cdot \text{s}$) is flowing through a 0.12-in- (= 0.010 ft) diameter 30-ft-long horizontal pipe steadily at an average velocity of 3.0 ft/s (Fig. 8–18). Determine (a) the head loss, (b) the pressure drop, and (c) the pumping power requirement to overcome this pressure drop.

SOLUTION The average flow velocity in a pipe is given. The head loss, the pressure drop, and the pumping power are to be determined.

Assumptions 1 The flow is steady and incompressible. 2 The entrance effects are negligible, and thus the flow is fully developed. 3 The pipe involves no components such as bends, valves, and connectors.

Properties The density and dynamic viscosity of water are given to be $\rho = 62.42 \text{ lbm/ft}^3$ and $\mu = 1.038 \times 10^{-3} \text{ lbm/ft} \cdot \text{s}$, respectively.

Analysis (a) First we need to determine the flow regime. The Reynolds number is

$$\text{Re} = \frac{\rho V_{\text{avg}} D}{\mu} = \frac{(62.42 \text{ lbm/ft}^3)(3 \text{ ft/s})(0.01 \text{ ft})}{1.038 \times 10^{-3} \text{ lbm/ft} \cdot \text{s}} = 1803$$

which is less than 2300. Therefore, the flow is laminar. Then the friction factor and the head loss become

$$f = \frac{64}{\text{Re}} = \frac{64}{1803} = 0.0355$$

$$h_L = f \frac{L}{D} \frac{V_{\text{avg}}^2}{2g} = 0.0355 \frac{30 \text{ ft}}{0.01 \text{ ft}} \frac{(3 \text{ ft/s})^2}{2(32.2 \text{ ft/s}^2)} = \mathbf{14.9 \text{ ft}}$$

(b) Noting that the pipe is horizontal and its diameter is constant, the pressure drop in the pipe is due entirely to the frictional losses and is equivalent to the pressure loss,

$$\Delta P = \Delta P_L = f \frac{L}{D} \frac{\rho V_{\text{avg}}^2}{2} = 0.0355 \frac{30 \text{ ft}}{0.01 \text{ ft}} \frac{(62.42 \text{ lbm/ft}^3)(3 \text{ ft/s})^2}{2} \left(\frac{1 \text{ lbf}}{32.2 \text{ lbm} \cdot \text{ft/s}^2} \right)$$

$$= 929 \text{ lbf/ft}^2 = 6.45 \text{ psi}$$

(c) The volume flow rate and the pumping power requirements are

$$\dot{V} = V_{\text{avg}} A_c = V_{\text{avg}} (\pi D^2/4) = (3 \text{ ft/s}) [\pi (0.01 \text{ ft})^2/4] = 0.000236 \text{ ft}^3/\text{s}$$

$$\dot{W}_{\text{pump}} = \dot{V} \Delta P = (0.000236 \text{ ft}^3/\text{s})(929 \text{ lbf/ft}^2) \left(\frac{1 \text{ W}}{0.737 \text{ lbf} \cdot \text{ft/s}} \right) = 0.30 \text{ W}$$

Therefore, power input in the amount of 0.30 W is needed to overcome the frictional losses in the flow due to viscosity.

Discussion The pressure rise provided by a pump is often listed by a pump manufacturer in units of head (Chap. 14). Thus, the pump in this flow needs to provide 14.9 ft of water head in order to overcome the irreversible head loss.

8-5 ■ TURBULENT FLOW IN PIPES

Most flows encountered in engineering practice are turbulent, and thus it is important to understand how turbulence affects wall shear stress. However, turbulent flow is a complex mechanism dominated by fluctuations, and despite tremendous amounts of work done in this area by researchers, the theory of turbulent flow remains largely undeveloped. Therefore, we must rely on experiments and the empirical or semi-empirical correlations developed for various situations.

Turbulent flow is characterized by random and rapid fluctuations of swirling regions of fluid, called **eddies**, throughout the flow. These fluctuations provide an additional mechanism for momentum and energy transfer. In laminar flow, fluid particles flow in an orderly manner along pathlines, and momentum and energy are transferred across streamlines by molecular diffusion. In turbulent flow, the swirling eddies transport mass, momentum, and energy to other regions of flow much more rapidly than molecular diffusion, greatly enhancing mass, momentum, and heat transfer. As a result, turbulent flow is associated with much higher values of friction, heat transfer, and mass transfer coefficients (Fig. 8-19).

Even when the average flow is steady, the eddy motion in turbulent flow causes significant fluctuations in the values of velocity, temperature, pressure, and even density (in compressible flow). Figure 8-20 shows the variation of the instantaneous velocity component u with time at a specified location, as can be measured with a hot-wire anemometer probe or other sensitive device. We observe that the instantaneous values of the velocity fluctuate about an average value, which suggests that the velocity can be expressed as the sum of an *average value* \bar{u} and a *fluctuating component* u' ,

$$u = \bar{u} + u' \tag{8-35}$$

This is also the case for other properties such as the velocity component v in the y -direction, and thus $v = \bar{v} + v'$, $P = \bar{P} + P'$, and $T = \bar{T} + T'$. The average value of a property at some location is determined by averaging it over a time interval that is sufficiently large so that the time average levels off to a constant. Therefore, the time average of fluctuating components is

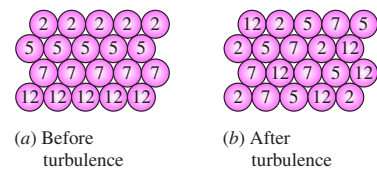


FIGURE 8-19

The intense mixing in turbulent flow brings fluid particles at different momentums into close contact and thus enhances momentum transfer.

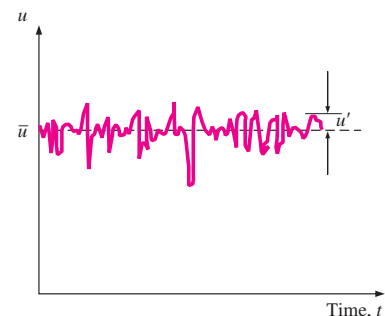


FIGURE 8-20

Fluctuations of the velocity component u with time at a specified location in turbulent flow.

zero, e.g., $\overline{u'} = 0$. The magnitude of u' is usually just a few percent of \bar{u} , but the high frequencies of eddies (in the order of a thousand per second) makes them very effective for the transport of momentum, thermal energy, and mass. In time-averaged *stationary* turbulent flow, the average values of properties (indicated by an overbar) are independent of time. The chaotic fluctuations of fluid particles play a dominant role in pressure drop, and these random motions must be considered in analyses together with the average velocity.

Perhaps the first thought that comes to mind is to determine the shear stress in an analogous manner to laminar flow from $\tau = -\mu d\bar{u}/dr$, where $\bar{u}(r)$ is the average velocity profile for turbulent flow. But the experimental studies show that this is not the case, and the shear stress is much larger due to the turbulent fluctuations. Therefore, it is convenient to think of the turbulent shear stress as consisting of two parts: the *laminar component*, which accounts for the friction between layers in the flow direction (expressed as $\tau_{\text{lam}} = -\mu d\bar{u}/dr$), and the *turbulent component*, which accounts for the friction between the fluctuating fluid particles and the fluid body (denoted as τ_{turb} and is related to the fluctuation components of velocity). Then the *total shear stress* in turbulent flow can be expressed as

$$\tau_{\text{total}} = \tau_{\text{lam}} + \tau_{\text{turb}} \tag{8-36}$$

The typical average velocity profile and relative magnitudes of laminar and turbulent components of shear stress for turbulent flow in a pipe are given in Fig. 8–21. Note that although the velocity profile is approximately parabolic in laminar flow, it becomes flatter or “fuller” in turbulent flow, with a sharp drop near the pipe wall. The fullness increases with the Reynolds number, and the velocity profile becomes more nearly uniform, lending support to the commonly utilized uniform velocity profile approximation for fully developed turbulent pipe flow. Keep in mind, however, that the flow speed at the wall of a stationary pipe is always zero (no-slip condition).

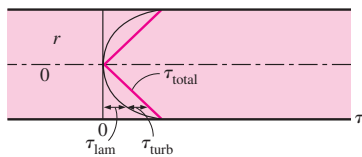
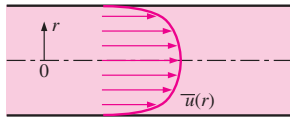


FIGURE 8–21 The velocity profile and the variation of shear stress with radial distance for turbulent flow in a pipe.

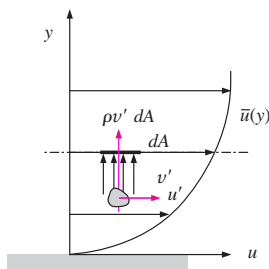


FIGURE 8–22 Fluid particle moving upward through a differential area dA as a result of the velocity fluctuation v' .

Turbulent Shear Stress

Consider turbulent flow in a horizontal pipe, and the upward eddy motion of fluid particles in a layer of lower velocity to an adjacent layer of higher velocity through a differential area dA as a result of the velocity fluctuation v' , as shown in Fig. 8–22. The mass flow rate of the fluid particles rising through dA is $\rho v' dA$, and its net effect on the layer above dA is a reduction in its average flow velocity because of momentum transfer to the fluid particles with lower average flow velocity. This momentum transfer causes the horizontal velocity of the fluid particles to increase by u' , and thus its momentum in the horizontal direction to increase at a rate of $(\rho v' dA)u'$, which must be equal to the decrease in the momentum of the upper fluid layer. Noting that force in a given direction is equal to the rate of change of momentum in that direction, the horizontal force acting on a fluid element above dA due to the passing of fluid particles through dA is $\delta F = (\rho v' dA)(-u') = -\rho u' v' dA$. Therefore, the shear force per unit area due to the eddy motion of fluid particles $\delta F/dA = -\rho u' v'$ can be viewed as the instantaneous turbulent shear stress. Then the **turbulent shear stress** can be expressed as

$$\tau_{\text{turb}} = -\rho \overline{u'v'} \tag{8-37}$$

where $\overline{u'v'}$ is the time average of the product of the fluctuating velocity components u' and v' . Note that $\overline{u'v'} \neq 0$ even though $\overline{u'} = 0$ and $\overline{v'} = 0$

(and thus $\overline{u'v'} = 0$), and experimental results show that $\overline{u'v'}$ is usually a negative quantity. Terms such as $-\rho\overline{u'v'}$ or $-\rho\overline{u'^2}$ are called **Reynolds stresses** or **turbulent stresses**.

Many semi-empirical formulations have been developed that model the Reynolds stress in terms of average velocity gradients in order to provide mathematical *closure* to the equations of motion. Such models are called **turbulence models** and are discussed in more detail in Chap. 15.

The random eddy motion of groups of particles resembles the random motion of molecules in a gas—colliding with each other after traveling a certain distance and exchanging momentum in the process. Therefore, momentum transport by eddies in turbulent flows is analogous to the molecular momentum diffusion. In many of the simpler turbulence models, turbulent shear stress is expressed in an analogous manner as suggested by the French mathematician Joseph Boussinesq (1842–1929) in 1877 as

$$\tau_{\text{turb}} = -\rho\overline{u'v'} = \mu_t \frac{\partial \bar{u}}{\partial y} \quad (8-38)$$

where μ_t is the **eddy viscosity** or **turbulent viscosity**, which accounts for momentum transport by turbulent eddies. Then the total shear stress can be expressed conveniently as

$$\tau_{\text{total}} = (\mu + \mu_t) \frac{\partial \bar{u}}{\partial y} = \rho(\nu + \nu_t) \frac{\partial \bar{u}}{\partial y} \quad (8-39)$$

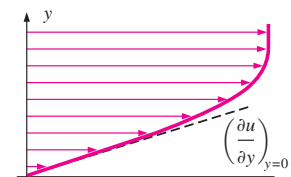
where $\nu_t = \mu_t/\rho$ is the **kinematic eddy viscosity** or **kinematic turbulent viscosity** (also called the *eddy diffusivity of momentum*). The concept of eddy viscosity is very appealing, but it is of no practical use unless its value can be determined. In other words, eddy viscosity must be modeled as a function of the average flow variables; we call this *eddy viscosity closure*. For example, in the early 1900s, the German engineer L. Prandtl introduced the concept of **mixing length** l_m , which is related to the average size of the eddies that are primarily responsible for mixing, and expressed the turbulent shear stress as

$$\tau_{\text{turb}} = \mu_t \frac{\partial \bar{u}}{\partial y} = \rho l_m^2 \left(\frac{\partial \bar{u}}{\partial y} \right)^2 \quad (8-40)$$

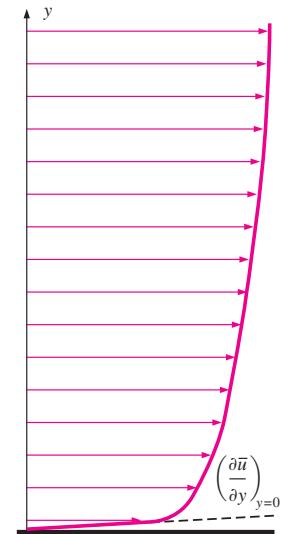
But this concept is also of limited use since l_m is not a constant for a given flow (in the vicinity of the wall, for example, l_m is nearly proportional to the distance from the wall) and its determination is not easy. Final mathematical closure is obtained only when l_m is written as a function of average flow variables, distance from the wall, etc.

Eddy motion and thus eddy diffusivities are much larger than their molecular counterparts in the core region of a turbulent boundary layer. The eddy motion loses its intensity close to the wall and diminishes at the wall because of the no-slip condition (u' and v' are identically zero at a stationary wall). Therefore, the velocity profile is very slowly changing in the core region of a turbulent boundary layer, but very steep in the thin layer adjacent to the wall, resulting in large velocity gradients at the wall surface. So it is no surprise that the wall shear stress is much larger in turbulent flow than it is in laminar flow (Fig. 8–23).

Note that molecular diffusivity of momentum ν (as well as μ) is a fluid property, and its value is listed in fluid handbooks. Eddy diffusivity ν_t (as well as μ_t), however, is *not* a fluid property, and its value depends on flow



Laminar flow



Turbulent flow

FIGURE 8-23

The velocity gradients at the wall, and thus the wall shear stress, are much larger for turbulent flow than they are for laminar flow, even though the turbulent boundary layer is thicker than the laminar one for the same value of free-stream velocity.

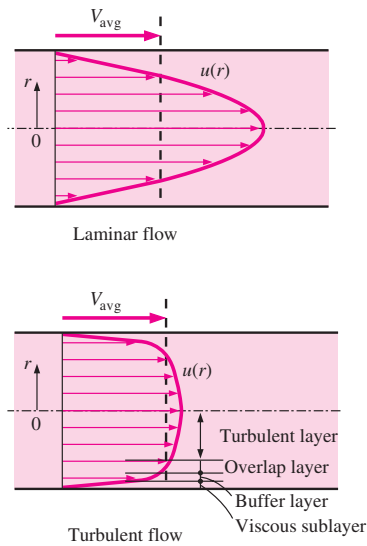


FIGURE 8-24 The velocity profile in fully developed pipe flow is parabolic in laminar flow, but much fuller in turbulent flow.

conditions. Eddy diffusivity ν_t decreases toward the wall, becoming zero at the wall. Its value ranges from zero at the wall to several thousand times the value of the molecular diffusivity in the core region.

Turbulent Velocity Profile

Unlike laminar flow, the expressions for the velocity profile in a turbulent flow are based on both analysis and measurements, and thus they are semi-empirical in nature with constants determined from experimental data. Consider fully developed turbulent flow in a pipe, and let u denote the time-averaged velocity in the axial direction (and thus drop the overbar from \bar{u} for simplicity).

Typical velocity profiles for fully developed laminar and turbulent flows are given in Fig. 8–24. Note that the velocity profile is parabolic in laminar flow but is much fuller in turbulent flow, with a sharp drop near the pipe wall. Turbulent flow along a wall can be considered to consist of four regions, characterized by the distance from the wall. The very thin layer next to the wall where viscous effects are dominant is the **viscous** (or **laminar** or **linear** or **wall**) sublayer. The velocity profile in this layer is very nearly *linear*, and the flow is streamlined. Next to the viscous sublayer is the **buffer layer**, in which turbulent effects are becoming significant, but the flow is still dominated by viscous effects. Above the buffer layer is the **overlap** (or **transition**) layer, also called the **inertial sublayer**, in which the turbulent effects are much more significant, but still not dominant. Above that is the **outer** (or **turbulent**) layer in the remaining part of the flow in which turbulent effects dominate over molecular diffusion (viscous) effects.

Flow characteristics are quite different in different regions, and thus it is difficult to come up with an analytic relation for the velocity profile for the entire flow as we did for laminar flow. The best approach in the turbulent case turns out to be to identify the key variables and functional forms using dimensional analysis, and then to use experimental data to determine the numerical values of any constants.

The thickness of the viscous sublayer is very small (typically, much less than 1 percent of the pipe diameter), but this thin layer next to the wall plays a dominant role on flow characteristics because of the large velocity gradients it involves. The wall dampens any eddy motion, and thus the flow in this layer is essentially laminar and the shear stress consists of laminar shear stress which is proportional to the fluid viscosity. Considering that velocity changes from zero to nearly the core region value across a layer that is sometimes no thicker than a hair (almost like a step function), we would expect the velocity profile in this layer to be very nearly linear, and experiments confirm that. Then the velocity gradient in the viscous sublayer remains nearly constant at $du/dy = u/y$, and the wall shear stress can be expressed as

$$\tau_w = \mu \frac{u}{y} = \rho \nu \frac{u}{y} \quad \text{or} \quad \frac{\tau_w}{\rho} = \frac{\nu u}{y} \tag{8-41}$$

where y is the distance from the wall (note that $y = R - r$ for a circular pipe). The quantity τ_w/ρ is frequently encountered in the analysis of turbulent velocity profiles. The square root of τ_w/ρ has the dimensions of velocity, and thus it is convenient to view it as a fictitious velocity called the **friction velocity** expressed as $u_* = \sqrt{\tau_w/\rho}$. Substituting this into Eq. 8–41, the velocity profile in the viscous sublayer can be expressed in dimensionless form as

Viscous sublayer:
$$\frac{u}{u_*} = \frac{yu_*}{\nu} \tag{8-42}$$

This equation is known as the **law of the wall**, and it is found to satisfactorily correlate with experimental data for smooth surfaces for $0 \leq yu_*/\nu \leq 5$. Therefore, the thickness of the viscous sublayer is roughly

Thickness of viscous sublayer:
$$y = \delta_{\text{sublayer}} = \frac{5\nu}{u_*} = \frac{25\nu}{u_\delta} \tag{8-43}$$

where u_δ is the flow velocity at the edge of the viscous sublayer, which is closely related to the average velocity in a pipe. Thus we conclude that *the thickness of the viscous sublayer is proportional to the kinematic viscosity and inversely proportional to the average flow velocity*. In other words, the viscous sublayer is suppressed and it gets thinner as the velocity (and thus the Reynolds number) increases. Consequently, the velocity profile becomes nearly flat and thus the velocity distribution becomes more uniform at very high Reynolds numbers.

The quantity ν/u_* has dimensions of length and is called the **viscous length**; it is used to nondimensionalize the distance y from the surface. In boundary layer analysis, it is convenient to work with nondimensionalized distance and nondimensionalized velocity defined as

Nondimensionalized variables:
$$y^+ = \frac{yu_*}{\nu} \quad \text{and} \quad u^+ = \frac{u}{u_*} \tag{8-44}$$

Then the law of the wall (Eq. 8-42) becomes simply

Normalized law of the wall:
$$u^+ = y^+ \tag{8-45}$$

Note that the friction velocity u_* is used to nondimensionalize both y and u , and y^+ resembles the Reynolds number expression.

In the overlap layer, the experimental data for velocity are observed to line up on a straight line when plotted against the logarithm of distance from the wall. Dimensional analysis indicates and the experiments confirm that the velocity in the overlap layer is proportional to the logarithm of distance, and the velocity profile can be expressed as

The logarithmic law:
$$\frac{u}{u_*} = \frac{1}{\kappa} \ln \frac{yu_*}{\nu} + B \tag{8-46}$$

where κ and B are constants whose values are determined experimentally to be about 0.40 and 5.0, respectively. Equation 8-46 is known as the **logarithmic law**. Substituting the values of the constants, the velocity profile is determined to be

Overlap layer:
$$\frac{u}{u_*} = 2.5 \ln \frac{yu_*}{\nu} + 5.0 \quad \text{or} \quad u^+ = 2.5 \ln y^+ + 5.0 \tag{8-47}$$

It turns out that the logarithmic law in Eq. 8-47 satisfactorily represents experimental data for the entire flow region except for the regions very close to the wall and near the pipe center, as shown in Fig. 8-25, and thus it is viewed as a *universal velocity profile* for turbulent flow in pipes or over surfaces. Note from the figure that the logarithmic-law velocity profile is quite accurate for $y^+ > 30$, but neither velocity profile is accurate in the buffer layer, i.e., the region $5 < y^+ < 30$. Also, the viscous sublayer appears much larger in the figure than it is since we used a logarithmic scale for distance from the wall.

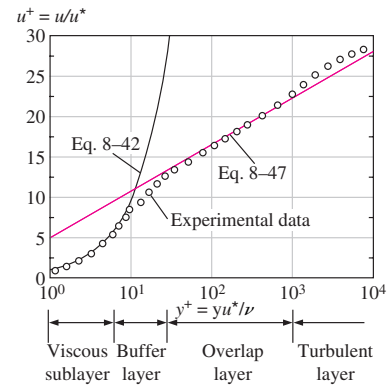


FIGURE 8-25 Comparison of the law of the wall and the logarithmic-law velocity profiles with experimental data for fully developed turbulent flow in a pipe.

A good approximation for the outer turbulent layer of pipe flow can be obtained by evaluating the constant B in Eq. 8-46 from the requirement that maximum velocity in a pipe occurs at the centerline where $r = 0$. Solving for B from Eq. 8-46 by setting $y = R - r = R$ and $u = u_{\max}$, and substituting it back into Eq. 8-46 together with $\kappa = 0.4$ gives

$$\text{Outer turbulent layer: } \frac{u_{\max} - u}{u_*} = 2.5 \ln \frac{R}{R - r} \quad (8-48)$$

The deviation of velocity from the centerline value $u_{\max} - u$ is called the **velocity defect**, and Eq. 8-48 is called the **velocity defect law**. This relation shows that the normalized velocity profile in the core region of turbulent flow in a pipe depends on the distance from the centerline and is independent of the viscosity of the fluid. This is not surprising since the eddy motion is dominant in this region, and the effect of fluid viscosity is negligible.

Numerous other empirical velocity profiles exist for turbulent pipe flow. Among those, the simplest and the best known is the **power-law velocity profile** expressed as

$$\text{Power-law velocity profile: } \frac{u}{u_{\max}} = \left(\frac{y}{R}\right)^{1/n} \quad \text{or} \quad \frac{u}{u_{\max}} = \left(1 - \frac{r}{R}\right)^{1/n} \quad (8-49)$$

where the exponent n is a constant whose value depends on the Reynolds number. The value of n increases with increasing Reynolds number. The value $n = 7$ generally approximates many flows in practice, giving rise to the term *one-seventh power-law velocity profile*.

Various power-law velocity profiles are shown in Fig. 8-26 for $n = 6, 8,$ and 10 together with the velocity profile for fully developed laminar flow for comparison. Note that the turbulent velocity profile is fuller than the laminar one, and it becomes more flat as n (and thus the Reynolds number) increases. Also note that the power-law profile cannot be used to calculate wall shear stress since it gives a velocity gradient of infinity there, and it fails to give zero slope at the centerline. But these regions of discrepancy constitute a small portion of flow, and the power-law profile gives highly accurate results for turbulent flow through a pipe.

Despite the small thickness of the viscous sublayer (usually much less than 1 percent of the pipe diameter), the characteristics of the flow in this layer are very important since they set the stage for flow in the rest of the pipe. Any irregularity or roughness on the surface disturbs this layer and affects the flow. Therefore, unlike laminar flow, the friction factor in turbulent flow is a strong function of surface roughness.

It should be kept in mind that roughness is a relative concept, and it has significance when its height ϵ is comparable to the thickness of the laminar sublayer (which is a function of the Reynolds number). All materials appear “rough” under a microscope with sufficient magnification. In fluid mechanics, a surface is characterized as being rough when the hills of roughness protrude out of the laminar sublayer. A surface is said to be smooth when the sublayer submerges the roughness elements. Glass and plastic surfaces are generally considered to be hydrodynamically smooth.

The Moody Chart

The friction factor in fully developed turbulent pipe flow depends on the Reynolds number and the **relative roughness** ϵ/D , which is the ratio of the

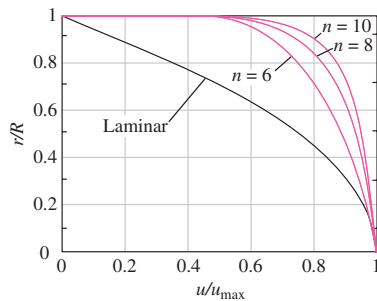


FIGURE 8-26 Power-law velocity profiles for fully developed turbulent flow in a pipe for different exponents, and its comparison with the laminar velocity profile.

mean height of roughness of the pipe to the pipe diameter. The functional form of this dependence cannot be obtained from a theoretical analysis, and all available results are obtained from painstaking experiments using artificially roughened surfaces (usually by gluing sand grains of a known size on the inner surfaces of the pipes). Most such experiments were conducted by Prandtl's student J. Nikuradse in 1933, followed by the works of others. The friction factor was calculated from the measurements of the flow rate and the pressure drop.

The experimental results obtained are presented in tabular, graphical, and functional forms obtained by curve-fitting experimental data. In 1939, Cyril F. Colebrook (1910–1997) combined the available data for transition and turbulent flow in smooth as well as rough pipes into the following implicit relation known as the **Colebrook equation**:

$$\frac{1}{\sqrt{f}} = -2.0 \log \left(\frac{\varepsilon/D}{3.7} + \frac{2.51}{\text{Re} \sqrt{f}} \right) \quad (\text{turbulent flow}) \quad (8-50)$$

We note that the logarithm in Eq. 8–50 is a base 10 rather than a natural logarithm. In 1942, the American engineer Hunter Rouse (1906–1996) verified Colebrook's equation and produced a graphical plot of f as a function of Re and the product $\text{Re} \sqrt{f}$. He also presented the laminar flow relation and a table of commercial pipe roughness. Two years later, Lewis F. Moody (1880–1953) redrew Rouse's diagram into the form commonly used today. The now famous **Moody chart** is given in the appendix as Fig. A–12. It presents the Darcy friction factor for pipe flow as a function of the Reynolds number and ε/D over a wide range. It is probably one of the most widely accepted and used charts in engineering. Although it is developed for circular pipes, it can also be used for noncircular pipes by replacing the diameter by the hydraulic diameter.

Commercially available pipes differ from those used in the experiments in that the roughness of pipes in the market is not uniform and it is difficult to give a precise description of it. Equivalent roughness values for some commercial pipes are given in Table 8–2 as well as on the Moody chart. But it should be kept in mind that these values are for new pipes, and the relative roughness of pipes may increase with use as a result of corrosion, scale buildup, and precipitation. As a result, the friction factor may increase by a factor of 5 to 10. Actual operating conditions must be considered in the design of piping systems. Also, the Moody chart and its equivalent Colebrook equation involve several uncertainties (the roughness size, experimental error, curve fitting of data, etc.), and thus the results obtained should not be treated as “exact.” It is usually considered to be accurate to ± 15 percent over the entire range in the figure.

The Colebrook equation is implicit in f , and thus the determination of the friction factor requires some iteration unless an equation solver such as EES is used. An approximate explicit relation for f was given by S. E. Haaland in 1983 as

$$\frac{1}{\sqrt{f}} \cong -1.8 \log \left[\frac{6.9}{\text{Re}} + \left(\frac{\varepsilon/D}{3.7} \right)^{1.11} \right] \quad (8-51)$$

The results obtained from this relation are within 2 percent of those obtained from the Colebrook equation. If more accurate results are desired, Eq. 8–51 can be used as a good *first guess* in a Newton iteration when using a programmable calculator or a spreadsheet to solve for f with Eq. 8–50.

TABLE 8–2

Equivalent roughness values for new commercial pipes*

Material	Roughness, ε	
	ft	mm
Glass, plastic	0 (smooth)	
Concrete	0.003–0.03	0.9–9
Wood stave	0.0016	0.5
Rubber, smoothed	0.000033	0.01
Copper or brass tubing	0.000005	0.0015
Cast iron	0.00085	0.26
Galvanized iron	0.0005	0.15
Wrought iron	0.00015	0.046
Stainless steel	0.000007	0.002
Commercial steel	0.00015	0.045

* The uncertainty in these values can be as much as ± 60 percent.

342
FLUID MECHANICS

Relative Roughness, ϵ/D	Friction Factor, f
0.0*	0.0119
0.00001	0.0119
0.0001	0.0134
0.0005	0.0172
0.001	0.0199
0.005	0.0305
0.01	0.0380
0.05	0.0716

* Smooth surface. All values are for $Re = 10^6$ and are calculated from the Colebrook equation.

FIGURE 8-27
The friction factor is minimum for a smooth pipe and increases with roughness.

We make the following observations from the Moody chart:

- For laminar flow, the friction factor decreases with increasing Reynolds number, and it is independent of surface roughness.
- The friction factor is a minimum for a smooth pipe (but still not zero because of the no-slip condition) and increases with roughness (Fig. 8-27). The Colebrook equation in this case ($\epsilon = 0$) reduces to the **Prandtl equation** expressed as $1/\sqrt{f} = 2.0 \log(Re\sqrt{f}) - 0.8$.
- The transition region from the laminar to turbulent regime ($2300 < Re < 4000$) is indicated by the shaded area in the Moody chart (Figs. 8-28 and A-12). The flow in this region may be laminar or turbulent, depending on flow disturbances, or it may alternate between laminar and turbulent, and thus the friction factor may also alternate between the values for laminar and turbulent flow. The data in this range are the least reliable. At small relative roughnesses, the friction factor increases in the transition region and approaches the value for smooth pipes.
- At very large Reynolds numbers (to the right of the dashed line on the chart) the friction factor curves corresponding to specified relative roughness curves are nearly horizontal, and thus the friction factors are independent of the Reynolds number (Fig. 8-28). The flow in that region is called *fully rough turbulent flow* or just *fully rough flow* because the thickness of the viscous sublayer decreases with increasing Reynolds number, and it becomes so thin that it is negligibly small compared to the surface roughness height. The viscous effects in this case are produced in the main flow primarily by the protruding roughness elements, and the contribution of the laminar sublayer is negligible. The Colebrook equation in the *fully rough zone* ($Re \rightarrow \infty$) reduces to the **von Kármán equation** expressed as $1/\sqrt{f} = -2.0 \log[(\epsilon/D)/3.7]$, which is explicit in f . Some authors call this zone *completely* (or *fully*) *turbulent flow*, but this is misleading since the flow to the left of the dashed blue line in Fig. 8-28 is also fully turbulent.

In calculations, we should make sure that we use the actual internal diameter of the pipe, which may be different than the nominal diameter. For example, the internal diameter of a steel pipe whose nominal diameter is 1 in is 1.049 in (Table 8-3).

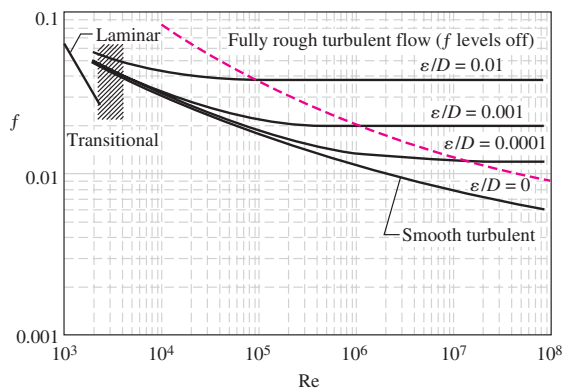


FIGURE 8-28
At very large Reynolds numbers, the friction factor curves on the Moody chart are nearly horizontal, and thus the friction factors are independent of the Reynolds number.

Types of Fluid Flow Problems

In the design and analysis of piping systems that involve the use of the Moody chart (or the Colebrook equation), we usually encounter three types of problems (the fluid and the roughness of the pipe are assumed to be specified in all cases) (Fig. 8–29):

1. Determining the **pressure drop** (or head loss) when the pipe length and diameter are given for a specified flow rate (or velocity)
2. Determining the **flow rate** when the pipe length and diameter are given for a specified pressure drop (or head loss)
3. Determining the **pipe diameter** when the pipe length and flow rate are given for a specified pressure drop (or head loss)

Problems of the *first type* are straightforward and can be solved directly by using the Moody chart. Problems of the *second type* and *third type* are commonly encountered in engineering design (in the selection of pipe diameter, for example, that minimizes the sum of the construction and pumping costs), but the use of the Moody chart with such problems requires an iterative approach unless an equation solver is used.

In problems of the *second type*, the diameter is given but the flow rate is unknown. A good guess for the friction factor in that case is obtained from the completely turbulent flow region for the given roughness. This is true for large Reynolds numbers, which is often the case in practice. Once the flow rate is obtained, the friction factor can be corrected using the Moody chart or the Colebrook equation, and the process is repeated until the solution converges. (Typically only a few iterations are required for convergence to three or four digits of precision.)

In problems of the *third type*, the diameter is not known and thus the Reynolds number and the relative roughness cannot be calculated. Therefore, we start calculations by assuming a pipe diameter. The pressure drop calculated for the assumed diameter is then compared to the specified pressure drop, and calculations are repeated with another pipe diameter in an iterative fashion until convergence.

To avoid tedious iterations in head loss, flow rate, and diameter calculations, Swamee and Jain proposed the following explicit relations in 1976 that are accurate to within 2 percent of the Moody chart:

$$h_L = 1.07 \frac{\dot{V}^2 L}{gD^5} \left\{ \ln \left[\frac{\epsilon}{3.7D} + 4.62 \left(\frac{\nu D}{\dot{V}} \right)^{0.9} \right] \right\}^{-2} \quad \begin{matrix} 10^{-6} < \epsilon/D < 10^{-2} \\ 3000 < Re < 3 \times 10^8 \end{matrix} \quad (8-52)$$

$$\dot{V} = -0.965 \left(\frac{gD^5 h_L}{L} \right)^{0.5} \ln \left[\frac{\epsilon}{3.7D} + \left(\frac{3.17 \nu^2 L}{gD^3 h_L} \right)^{0.5} \right] \quad Re > 2000 \quad (8-53)$$

$$D = 0.66 \left[\epsilon^{1.25} \left(\frac{L \dot{V}^2}{gh_L} \right)^{4.75} + \nu \dot{V}^{9.4} \left(\frac{L}{gh_L} \right)^{5.270.04} \right]^{-0.04} \quad \begin{matrix} 10^{-6} < \epsilon/D < 10^{-2} \\ 5000 < Re < 3 \times 10^8 \end{matrix} \quad (8-54)$$

Note that all quantities are dimensional and the units simplify to the desired unit (for example, to m or ft in the last relation) when consistent units are used. Noting that the Moody chart is accurate to within 15 percent of experimental data, we should have no reservation in using these approximate relations in the design of piping systems.

TABLE 8–3

Standard sizes for Schedule 40 steel pipes

Nominal Size, in	Actual Inside Diameter, in
$\frac{1}{8}$	0.269
$\frac{1}{4}$	0.364
$\frac{3}{8}$	0.493
$\frac{1}{2}$	0.622
$\frac{3}{4}$	0.824
1	1.049
$1\frac{1}{2}$	1.610
2	2.067
$2\frac{1}{2}$	2.469
3	3.068
5	5.047
10	10.02

Problem type	Given	Find
1	L, D, \dot{V}	ΔP (or h_L)
2	$L, D, \Delta P$	\dot{V}
3	$L, \Delta P, \dot{V}$	D

FIGURE 8–29 The three types of problems encountered in pipe flow.